





Article

A New Equivalent Circuit Model Parametrization Methodology Based on Current Pulse Tests for Different Battery Technologies

Oier Arregi ^{1,*}, Eneko Agirrezabala ¹, Unai Iraola ¹, Aitor Milo ², Josu Yeregui ¹, Unai Nogueras ¹, Roberto Sánchez ³ and Iñigo Gil ³

¹ Electronics and Informatics Department, Faculty of Engineering, Mondragon Unibertsitatea, Loramendi 4, 20500 Mondragón, Gipuzkoa, Spain; eagirrezabala@mondragon.edu (E.A.); uiraola@mondragon.edu (U.I.); josu.yeregui@alumni.mondragon.edu (J.Y.); unai.nogueras@alumni.mondragon.edu (U.N.)

² Ikerlan Technology Research Centre, Basque Research and Technology Alliance (BRTA), P.º J.M. Arizmendiarieta, 2, 20500 Mondragón, Spain; amilo@ikerlan.es

³ Department of Electrical Drives and Energy, Orona S. Coop., 20120 Hernani, Spain; rsanchezmo@orona-group.com (R.S.); igil@orona-group.com (I.G.)

* Correspondence: oarregi@mondragon.edu

Abstract: With growing global commitment to renewable energy generation, the role of energy storage systems has become a central issue in traction power applications, such as electric vehicles, trains, and elevators. To achieve the optimal integration of batteries in such applications, without unnecessary oversizing, improvements in the process of battery selection are needed. Specifically, it is necessary to develop models able to predict battery performance for each particular application. In this paper, a methodology for the parametrization of a battery equivalent circuit model (ECM) based on capacity and pulse tests is presented. The model can be extrapolated to different battery technologies, and was validated by comparing simulations and experimental tests with lead-acid and lithium-ion batteries.

Keywords: lead-acid battery; lithium ion battery; parameter identification; equivalent circuit model (ECM)



Citation: Arregi, O.; Agirrezabala, E.; Iraola, U.; Milo, A.; Yeregui, J.; Nogueras, U.; Sánchez, R.; Gil, I. A New Equivalent Circuit Model Parametrization Methodology Based on Current Pulse Tests for Different Battery Technologies. *Energies* **2021**, *14*, 7255. <https://doi.org/10.3390/en14217255>

Academic Editor: Cai Shen

Received: 13 October 2021

Accepted: 1 November 2021

Published: 3 November 2021

Publisher's Note: MDPI stays neutral with regard to jurisdictional claims in published maps and institutional affiliations.



Copyright: © 2021 by the authors. Licensee MDPI, Basel, Switzerland. This article is an open access article distributed under the terms and conditions of the Creative Commons Attribution (CC BY) license (<https://creativecommons.org/licenses/by/4.0/>).

1. Introduction

Growing global energy consumption and dependency on fossil fuels have caused unprecedented warming of the climate system. Addressing the resultant environmental problems has necessitated a shift in energy generation policies, with governments around the world making a clear commitment to renewable energies [1]. Renewable energies have many advantages when compared to a fossil fuel-driven economy. However, the dependence of these energy sources on climate conditions, and the subsequent irregularity of energy generation, is a significant drawback that must be addressed. This irregularity necessitates the use of energy storage systems, and in particular, batteries, to store energy in peak generation periods for later use when generation is low.

Battery technologies are constantly evolving, and as a result there has been increased uptake in their usage [2]. Electromobility applications are a clear example of this. The use of batteries in traction applications carries several benefits. On the one hand, use in electric vehicles reduces their overall energy consumption by regenerating energy during braking [3]. On the other hand, in grid-connected transport applications, such as elevators or rail traction, where power consumption is not constant, i.e., where power demand has transient consumption and regeneration peaks, the addition of an energy storage system considerably reduces contracted power and energy consumption [4,5]. The problem, however, is that energy storage requirements change depending on the technology that is being used and the characteristics of the application, and thus the battery selected will also change. Moreover, this battery selection process is costly and time-consuming.

The first step of battery selection is the identification of an appropriate technology for each specific application. To do this, different battery technologies must be analyzed and compared [6,7]. Once the battery selection is finalized, it is then necessary to obtain an accurate model.

Most of the papers found in the literature present a methodology for a specific battery technology, where the selected battery model and the proposed test are specifically designed for it. Taking into account the fact that, in the literature, there are several battery models, and some of them are used for different battery technologies, it seems interesting to be able to parametrize different batteries using the same methodology.

This paper presents a methodology to obtain a voltage prediction behavioral parametrizable model for different battery technologies, such as lithium-ion or lead-acid, which are the most widely used technologies at present. This model is designed to be suitable for any application scenario regardless of the technology used, and takes into account the following operational conditions: the state of charge (SOC), the working current rate, the state of health (SOH), and the working temperature.

In the following sections, each of the steps of the methodology used to develop the parametrizable behavioral model is outlined, including the selection of the battery model, the parametrization tests, as well as the comparative process between simulation and experimental tests.

2. Methodology

The aim of this research is to predict battery voltage behavior under different working conditions. To this end, the first step was the selection of the most suitable battery model.

The next step was to select the battery characterization test and the parameter extraction method used to estimate the variables of the model.

Finally, and based on the results obtained in previous tests, the model was validated by applying a real traction application consumption profile to the battery, and comparing the estimated terminal voltages to those measured.

The methodology followed is set out in Figure 1.

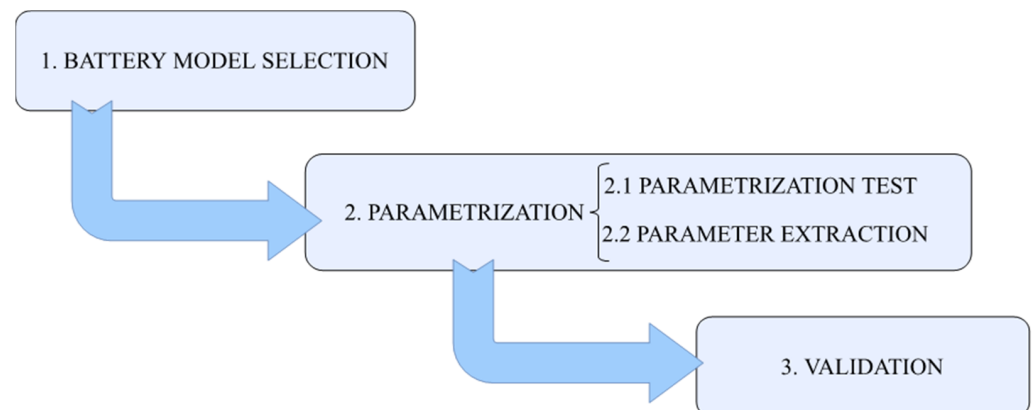


Figure 1. Battery model parametrization methodology.

3. Battery Model

Batteries are complex electrochemical systems due to the combination of different dynamic variables such as electrical behavior, thermal behavior, and degradation. These dynamics are determined by the following state variables: state of charge (SOC), state of health (SOH), current rate, and temperature. When analyzing battery-based storage systems, such as in the work of [8,9], the use of a battery model able to represent the dynamics of the cells becomes crucial. Such models allow for the prediction and optimization of the behavior of the system under different conditions.

Improvements in software capacity and computing power in the last few decades mean that the modeling and simulation of batteries has become faster and cheaper. A wide variety of battery models with different degrees of complexity have been developed, and these can be classified into three groups: electrochemical models, mathematical models, and electrical models.

Electrochemical models [10,11] are mainly used to optimize physical aspects of battery design, characterize the main power generation mechanisms and identify design parameters from a macroscopic and microscopic point of view. These models are based on partial differential equations, taking into consideration the movement and chemical reactions of particles inside the battery. Although this approach has the highest level of accuracy, it is the most time-consuming and complex model [12]. In recent studies it can be observed that the computational cost of electrochemical models is decreasing due to the simplification of the models; in some cases, such as single-particle models, they can even be used in online applications [13].

Mathematical models [14,15] use empirical equations to predict the system behavior, such as the battery capacity or battery efficiency. They have an abstract practical meaning and they are valid only for specific applications. Moreover, the relative error in the results of these kinds of models ranges from around 5% to 20% [12].

Electrical models, also known as ECMs (equivalent circuit models), predict battery behavior by using linear elements such as voltage sources, resistances or capacitors, and can also be combined with other electrical circuits when simulating or designing. Furthermore, these models are more intuitive and simpler to solve. Although they are not the most accurate models, the relative error in their results is low and usually varies between 1% and 5%. Of these three groups, electrical models provide the optimum balance between accuracy and complexity [12], which is why they are the most widely used models in different areas. One such example is the case of a BMS (battery management system) for an electrical vehicle, offering high precision in dynamic simulations [16,17].

Several kinds of ECMs can be seen in the literature for use in different battery technologies [18,19]. In this paper, we have focused on the ones presented in the Figure 2. These ECMs are the most common, and are used in different battery technologies.

The IR model or internal resistance model, shown in Figure 2a, uses a resistance, R_o , that represents the internal resistance of the battery, and an ideal voltage source, VOC , that represents the OCV (open-circuit voltage). Both values are functions of SOC and battery temperature. In addition, with increased usage and the resulting SOH reduction, the internal resistance of a cell increases [9]. Although this model is used when modeling lead-acid batteries for some applications, it cannot represent battery transient behaviors, and hence it is not suitable for an accurate dynamic estimation of the SOC and the voltage [20].

The OTC model or one-time constant model, shown in Figure 2b, adds a parallel RC branch in series with the internal resistance previously mentioned. Thus, the model is able to represent the transient behavior of the battery [21,22]. However, as shown in the work of [20], when monitoring the output voltage while the current is zero (without load), the battery presented a significant difference between short- and long-term transient behavior. For this reason, the OTC model is not able to accurately represent the dynamics of a battery. However, it is widely used in lead-acid technology [23].

The TTC model, or two-time constant model, shown in Figure 2c, solves this problem by adding another parallel RC branch. By doing so, the first RC branch describes the short-term behavior of the battery, while the second RC branch describes the long-term behavior of the battery [24–26].

As stated in [27], the IR model is too simple to be able to represent battery dynamics. Thus, this model is not suitable for predicting the SOC value in a dynamic system. The OTC model describes the transient behavior of the battery; however, it cannot accurately predict fast dynamics, especially in aging batteries [27]. Hence, is not an accurate model for lithium-ion batteries, even if it is valid for use in lead-acid technology.

In conclusion, it is necessary to have at least two parallel RC branches in order to properly describe fast and slow dynamics. According to the analysis performed by [12], even if it is possible to add more RC branches, the TTC model offers the best compromise between accuracy and complexity. Hence, the ECM with two time constants was selected for further analysis.

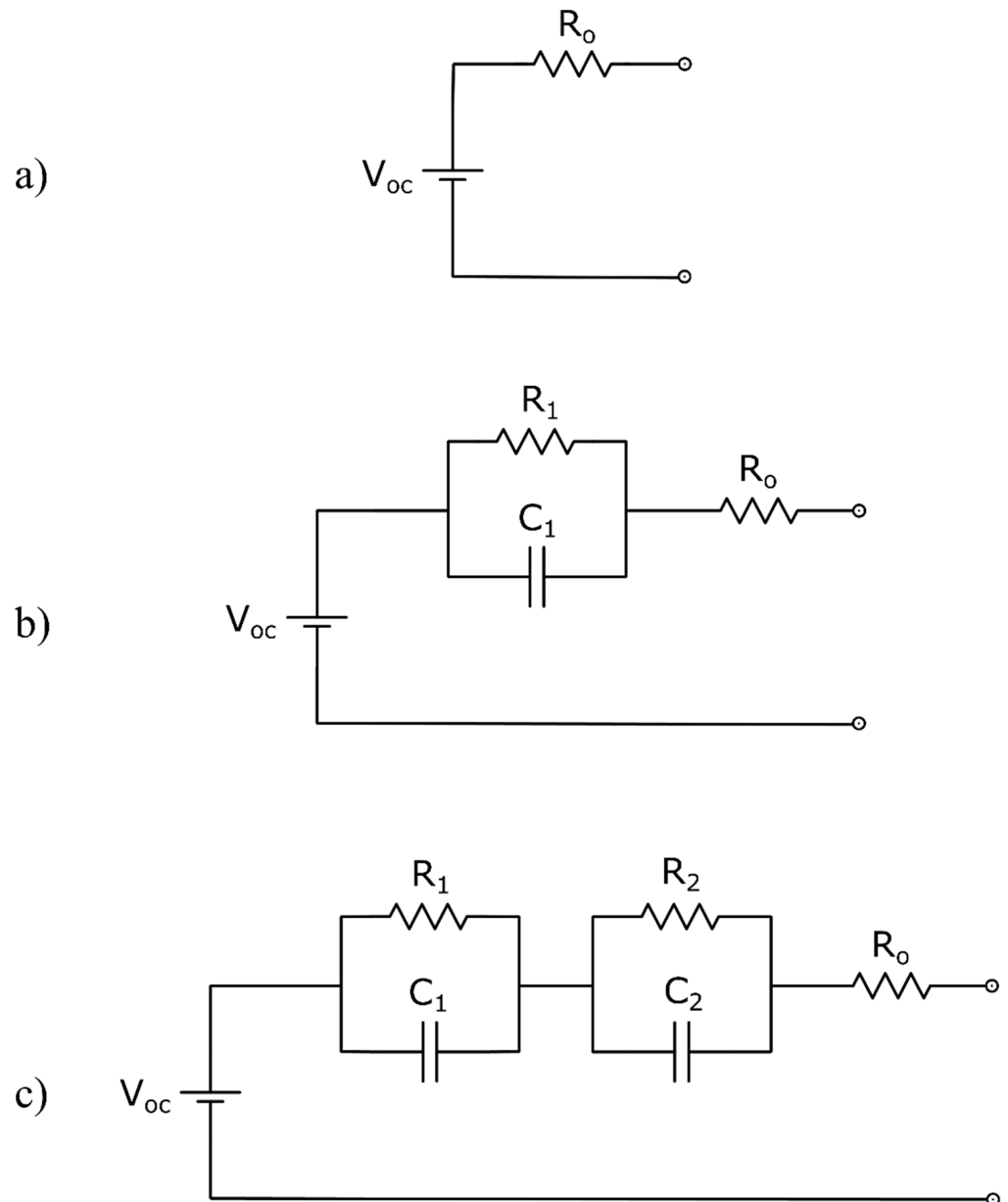


Figure 2. Battery ECM diagrams. (a) Internal resistance model, (b) one-time constant model, (c) two-time constant model.

4. Parametrization Test

Different battery parametrization tests can be performed to obtain the variables of the model. These parameters can be identified by making measurements in the frequency domain or in the time domain.

Electrochemical impedance spectroscopy (EIS) or the AC impedance method is the most extended frequency domain method. EIS studies the system voltage response to the application of a periodic small-amplitude sinusoidal AC signal. An impedance spectrum

analyzer is required to perform this measurement, which makes it a simple and accurate method, but also expensive [28].

With respect to the time domain method, the current and voltage are measured simultaneously in order to identify the impedances of the model. This method does not require specific equipment, and is the method that was selected for this paper. To analyze the voltage response of the battery, pulse tests, also known as dynamic tests, are applied. In these tests, various charge and discharge current patterns are applied along the SOC. To identify the most suitable pulse test pattern, two main pulse test methods were compared.

In the first method, presented in [17], charge and discharge pulses are divided into two parts along the SOC. On the one hand, pulses of 1% of the capacity are made when the SOC is above 90% and below 10%. On the other hand, pulses of 5% of SOC are made when the SOC is between 90% and 10%. In both cases, the current has an amplitude of 1C; one-hour rest periods are applied for 1% capacity pulses and four hours rest for 5% capacity pulses, to ensure voltage and current stabilization.

In the second method, presented in [27], 10 charge sequences and 10 discharge sequences are applied following the same pattern. Three different parts are distinguished in each sequence. In the first part, three consecutive pulses with 5 s on and off periods are applied before and after each modeling pulse, to evaluate the ohmic resistance change. In the second part, a modeling pulse with a C/4 current amplitude and 5% of SOC duration is applied to identify the parameters of ECM, followed by three consecutive pulses for ohmic resistance change and a one-hour rest period. In the third part, five verification pulses are applied to verify the ECM parameters using different current rates from the one used for the parameter identification. This also identifies the state of power (SOP) under different operational conditions. Table 1 shows a comparison between the two methods.

Table 1. Comparison between two different pulse test methods.

Symbol	[17] Method	[27] Method
Test duration	≈85 h	≈65 h
Analyzed current rates	1C	C/4, C/2, C, 1.5C, and 2C
Complexity	Lower complexity	Higher complexity
Max. error	1.2%	0.9%

The main difference between both methods is the analyzed current rate. For the case of an application wherein the current is constant, the method presented in [17] would be the best choice, due to its simplicity. However, in an application where the current range varies, analyzing only one rate can be a drawback. For example, in the case of an elevator or an electric vehicle, where the current demand is not constant, the best method would be that presented in [27]. Although the complexity of this method is greater, the analyzed current rate range covers most of the working currents of the application.

In this paper, the method presented in [27] was selected as a baseline. However, it was considered that to estimate the Ro value it was not necessary to separate the internal resistance calculation from the calculation of the rest of the parameters of the ECM. This is because the estimation in both cases was very similar. Taking this into account, the profile for internal resistance calculation was deleted. The implemented pulse test method procedure for the ECM parametrization is shown in Figure 3.

As can be seen in Figure 3, the test began with the battery fully discharged (SOC = 0%) and five charge pulses with different current rates (2% of the capacity each pulse) were applied. After each pulse, the battery was left resting for 30 min to stabilize the voltage and obtain the relaxation curves for ECM parameter estimation. This pattern was repeated ten times, reaching an SOC value of 100%. When the battery was fully charged, five discharge pulses with different current rates, supposing 2% of the capacity, were applied. As in the previous case, this pattern was repeated ten times, reaching an SOC value of 0%. The rest time between pulses for this case was also 30 min.

It is important to note that a capacity test was performed at the C/20 charging rate before the pulse test. Thus, the SOH of the battery was estimated and the OCV curves were obtained. These variables were later used to obtain ECM parameters. The pulse test current profile is summarized in Figure 4, where the initial capacity test and the pulses described in Figure 3 are shown.

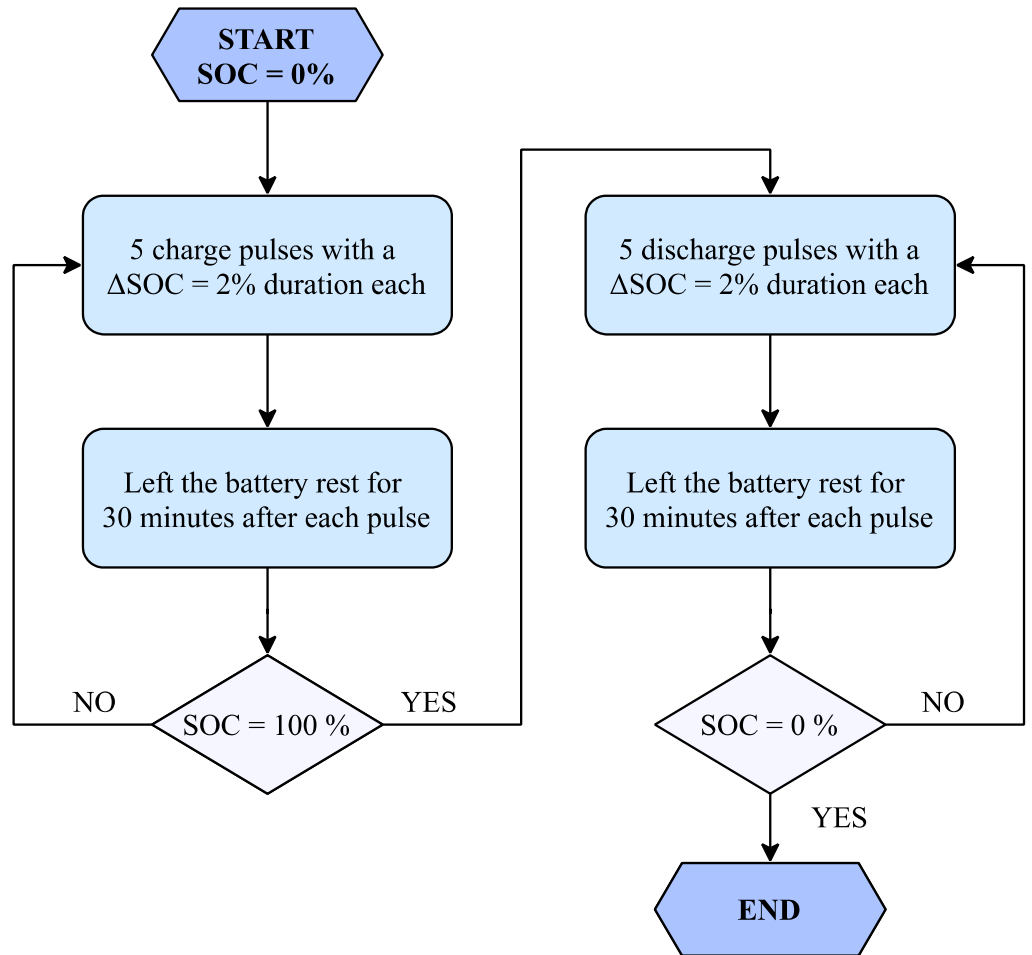


Figure 3. Implemented pulse test method procedure for the ECM parametrization.

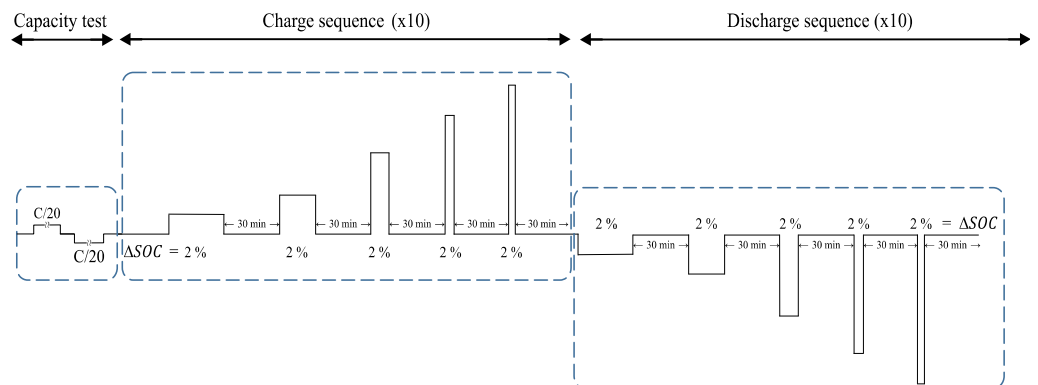


Figure 4. Implemented pulse test current profile used to obtain ECM parameters.

5. Parameter Extraction

Once the tests were finalized, it was necessary to identify a parameter extraction procedure. This procedure was divided into three parts.

In the first part, a voltage source and an electronic load were used to perform the capacity and pulse tests described above. After applying current pulses, the battery voltage relaxation curves were obtained.

In the second part, these data were filtered and the ECM parameters were identified. By doing so, ECM values were obtained for the whole range of the SOC and the different tested current rates.

In the third part, the model was validated by estimating the voltage response of the battery for a specific input current profile and comparing it with the real response of the battery.

The Figure 5 sets out the procedure followed for the parameter extraction and estimation.

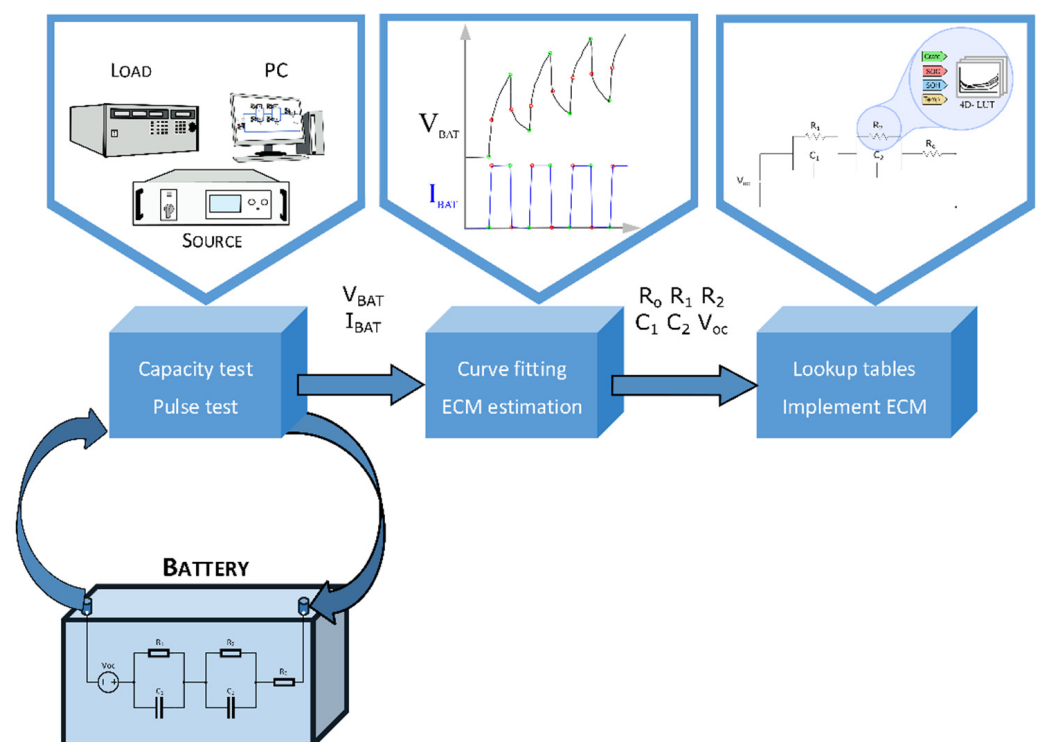


Figure 5. Procedure followed for parameter extraction and estimation.

In this procedure, the battery was first tested with the previously defined capacity test, and the voltage and current measurements were taken. The capacity was obtained using the coulomb counting method, which is based on counting the discharged current. Once the capacity was calculated, the SOH was estimated via Equation (1).

$$SOH = \frac{C_{max}}{C_n} \times 100 \quad (1)$$

where C_{max} is the measured battery capacity and C_n is the nominal battery capacity.

As well as providing the SOH estimation, the OCV was also obtained from the capacity test. As it is a key step when parametrizing ECMs, it is necessary to obtain an accurate estimation of this. The OCV was obtained by interpolating the charging and discharging voltage curves measured in the test shown in Figure 6.

Once the capacity test had been performed and the SOH and OCV curves were estimated, the battery was tested with the previously defined pulse test, and the current and voltage measurements were taken. After measuring the voltage dynamics of the battery,

it was necessary to identify the pulse and relaxation events in the automatically obtained data to estimate the ECM element values. To do so, a code that follows the procedure shown in Figure 7 was created. The relaxation curves were obtained by identifying the beginnings and ends of the current pulses, and the parameters of the battery model were estimated.

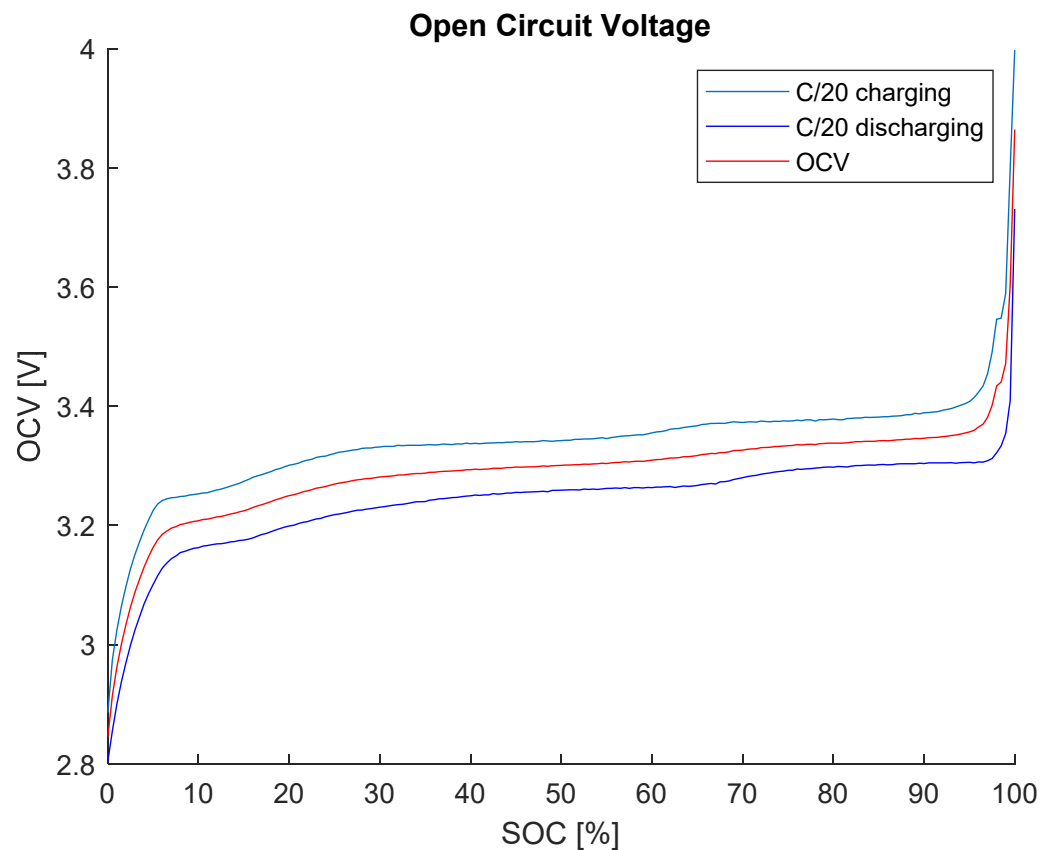


Figure 6. Lithium-ion battery OCV curve.

The implemented code analyzes the current profile and identifies the current pulses. By doing so, the voltage relaxation curves as well as voltage drops are isolated from the rest of the curves. The relaxation curves show the battery voltage measurement when the battery is at rest, so the curves consist of the period from the end of each current pulse to the beginning of the next one. An example of this filtering is shown in Figure 8.

Once the pulse events were filtered, based on the technique described in [27], the internal resistance value was estimated taking into account the voltage drop at the first instant of the pulse. Then, the least square method was applied to the voltage relaxation to estimate the rest of the ECM parameter values. A comparison between the real relaxation curve and the curve calculated with the least square method is shown in Figure 9.

Obtaining the values of the parameters v_x and τ_x with the equation presented in Figure 9, it is possible to estimate the values of the resistances and the capacitors of the two time constant models with Equations (2) and (3), where R_x and C_x are the resistance and the capacitor of time constant x , respectively, and i_{pulse} and T_{pulse} are the current pulse and its duration.

$$R_x = \frac{v_x}{\left(1 - e^{-\frac{T_{\text{pulse}}}{\tau_x}}\right) i_{\text{pulse}}} \quad (2)$$

$$C_x = \frac{\tau_x}{R_x} \quad (3)$$

After identifying the equivalent circuit parameters for all the relaxation curves, the results were implemented in the model. The parameters of the model vary depending on

the operating conditions, taking into account the current rate and the SOC of the battery for the SOH and the temperature at time of testing. Battery model parameters are known to vary due to changes in temperature and aging [29,30]. By repeating this methodology for different SOHs, a more accurate model can be obtained, which takes into account the current rate, the SOC, and the SOH of the battery. Although it is not validated in this paper, this methodology can be also used for different temperatures.

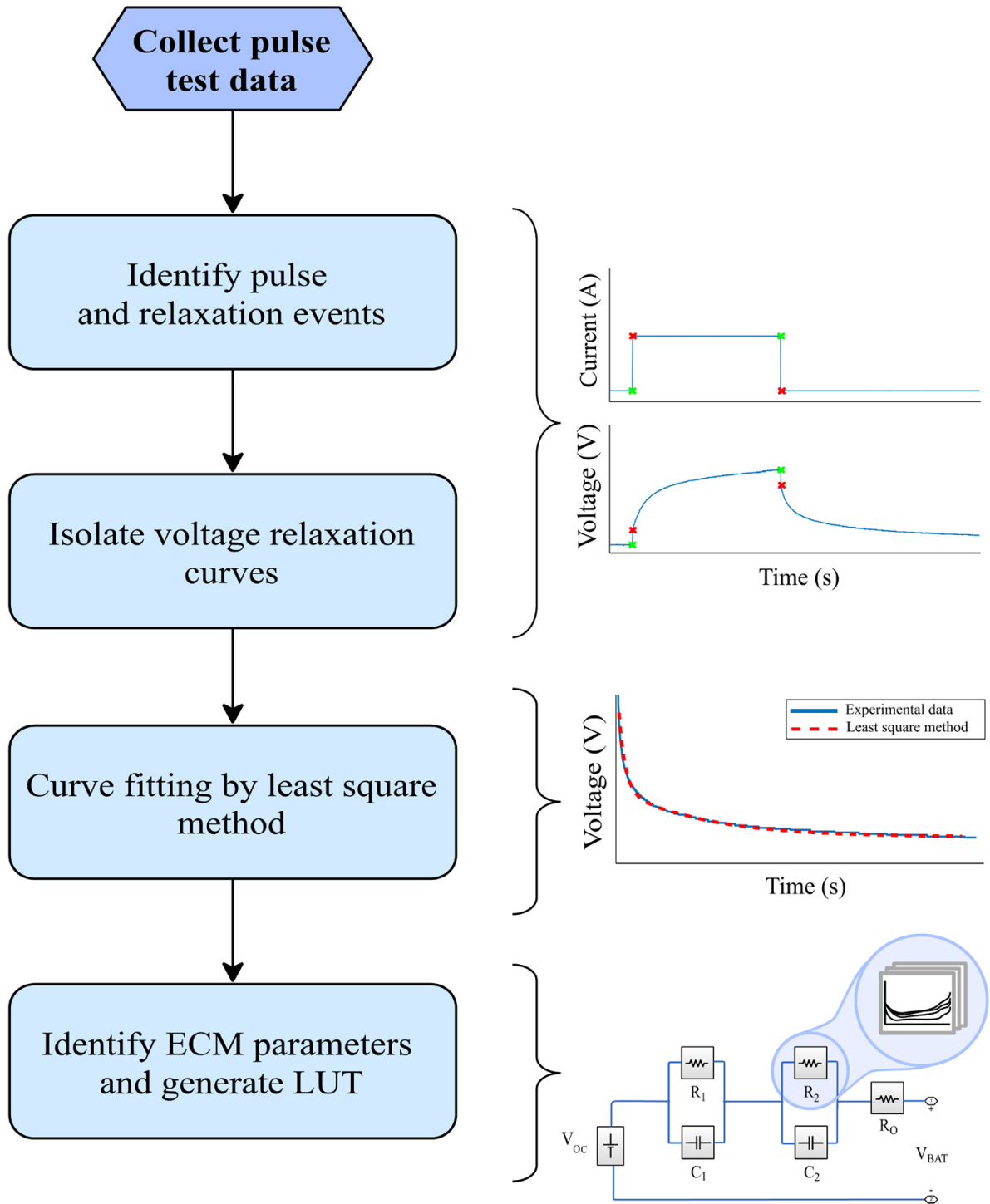


Figure 7. Followed procedure in the ECM parameter identification code.

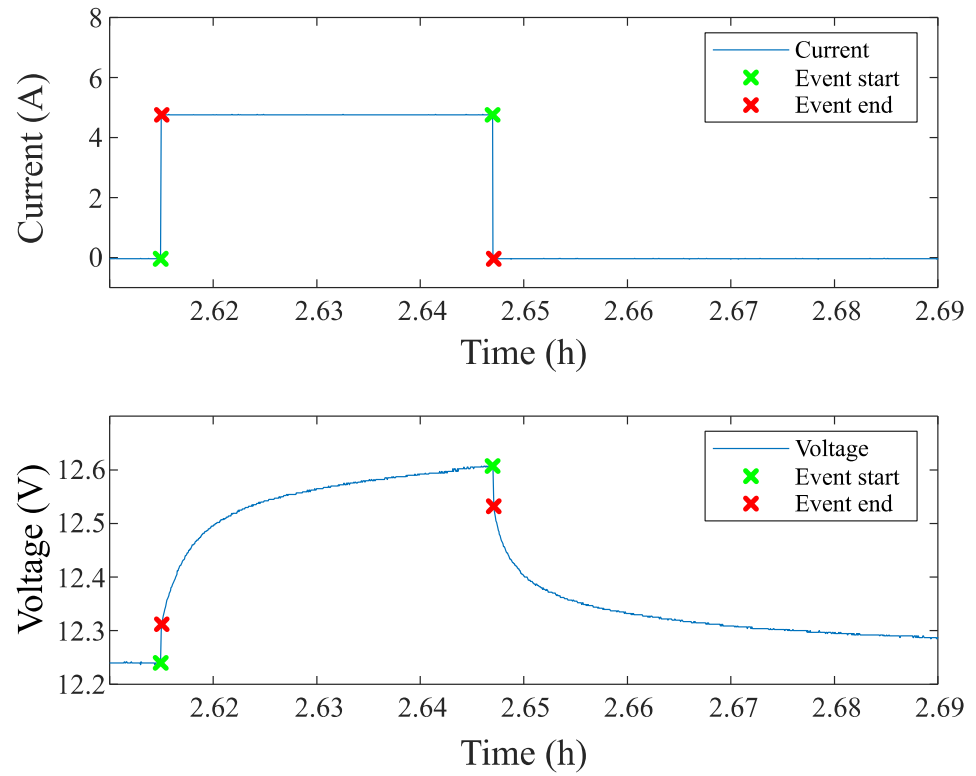


Figure 8. Identification of current pulses and voltage relaxation events.

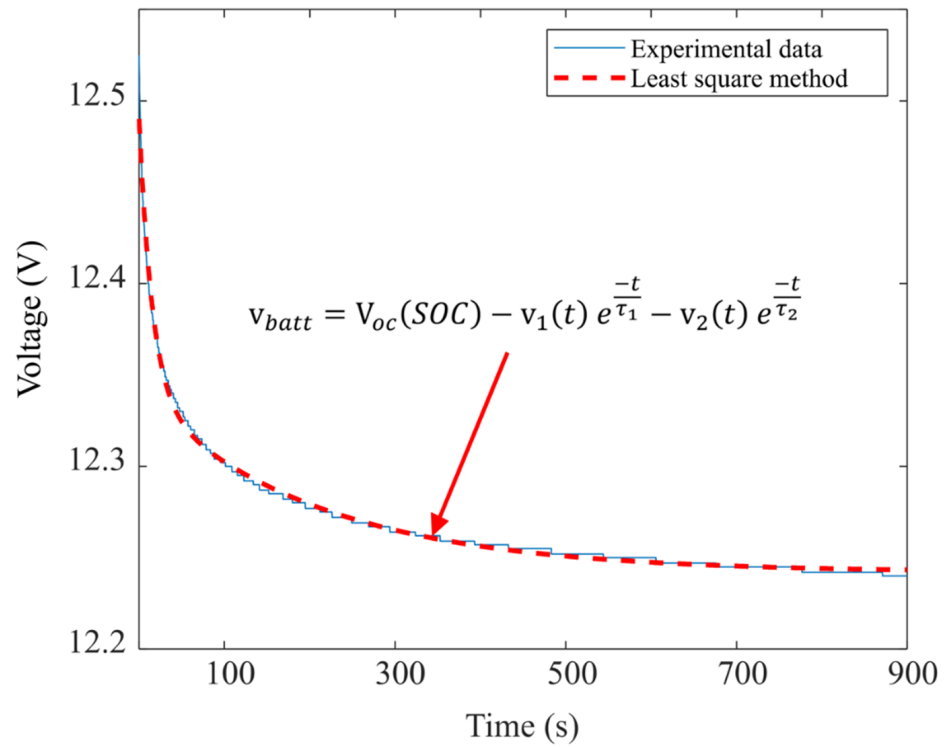


Figure 9. Voltage relaxation curve characterization using least square method.

6. Model Validation

To validate the behavioral model and the proposed parameter extraction method, a validation test was carried out. This test is based on the real energy consumption of an

elevator, where the battery input is the current demand. This current demand was applied to the battery with an SOC value of 50%.

This section sets out the results from the parameter extraction and the validation tests, in which the real and simulated output terminal voltages of the battery were compared.

The first technology to be analyzed was a lithium-ion battery. The tested battery was an LYP40AHA from Thunder Sky Winston with an SOH of 100% [31], which was tested in the manufacturer-recommended operating voltage range of 2.8 V to 4 V. The results from the parameter extraction and validation tests are shown in Figures 10–12.

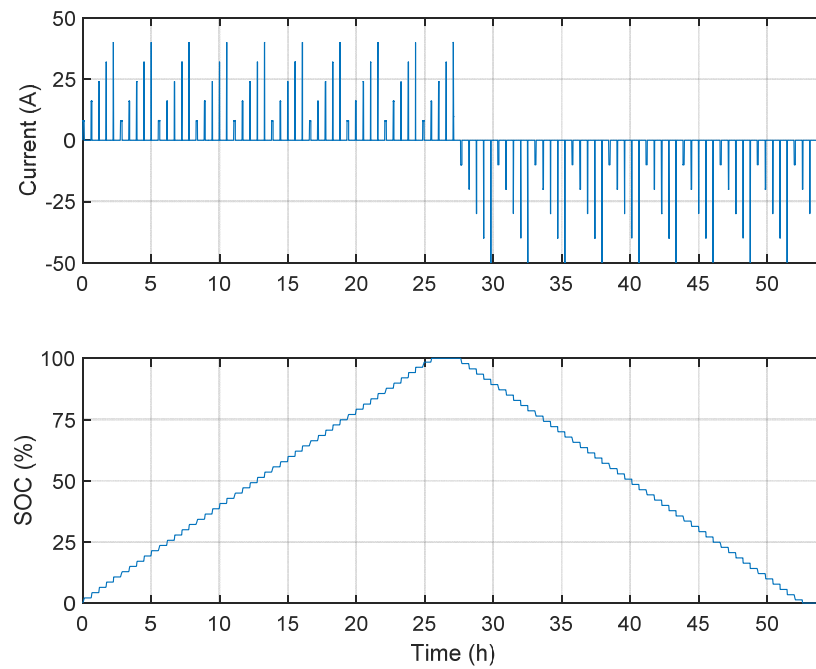


Figure 10. Lithium-ion battery parameter extraction test current and SOC.

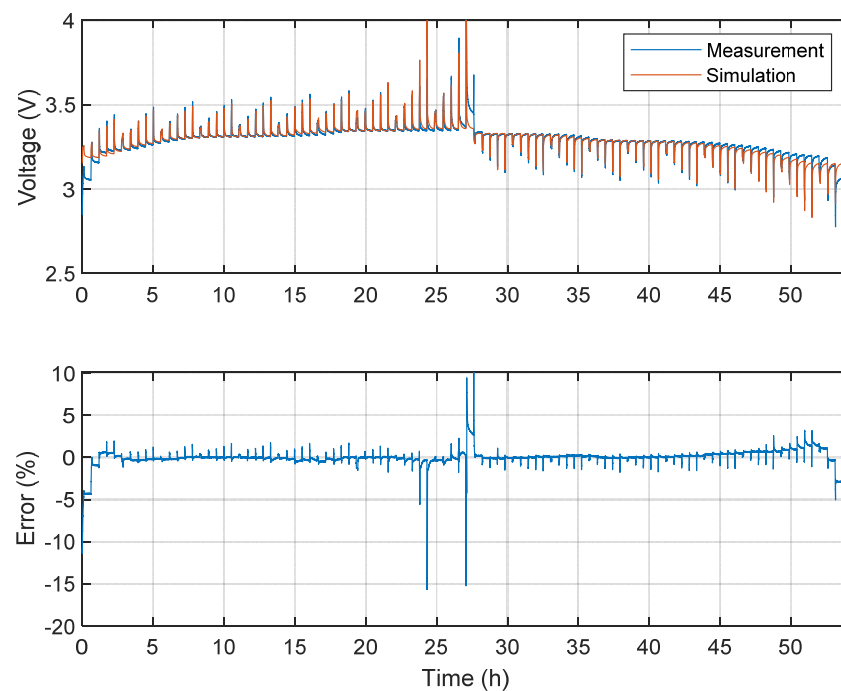


Figure 11. Lithium-ion battery parameter extraction test voltage response.

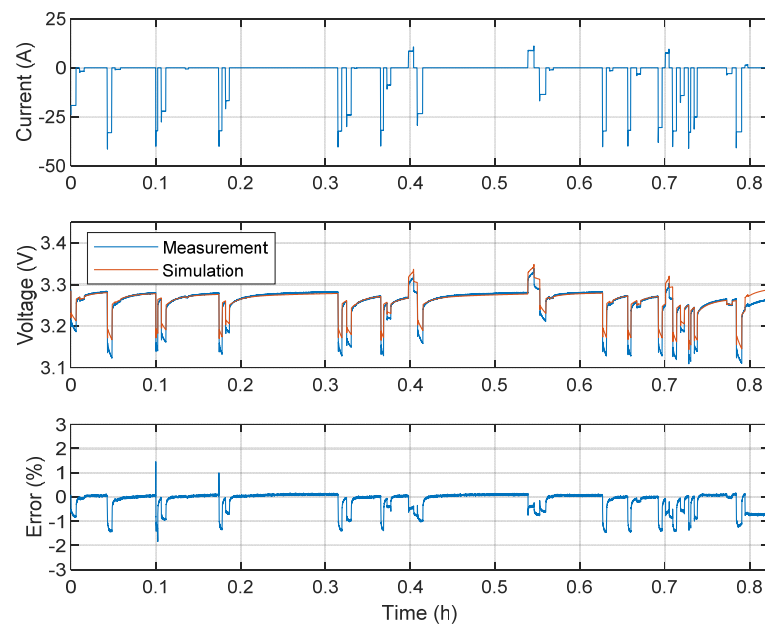


Figure 12. Lithium-ion battery validation test.

As can be seen in Figure 11, the best accuracy was obtained in an SOC range between 20 and 80%, which is the most interesting range for traction applications [32]. In this range, the maximum relative error obtained in the charge sequence was 1.75%, and 1.8% in the discharge sequence. The discharge sequence error was greater because the discharge rates of the validation test were higher than those of charging, with maximum errors of 1.85% and 0.75% in the discharge and charge sequences, respectively.

The second technology analyzed was the lead-acid battery, using the model NPC24-12 of 24 Ah from YUASA [33]. The minimum voltage recommended by the manufacturer is 10.5 V, the maximum voltage 14.5 V, and the floating voltage 13.65 V. In this battery model, the parametrization was carried out using two different SOHs; a new battery (100% SOH) and an aged battery (40% SOH). The results obtained in the validation tests for both cases are set out in Figures 13 and 14.

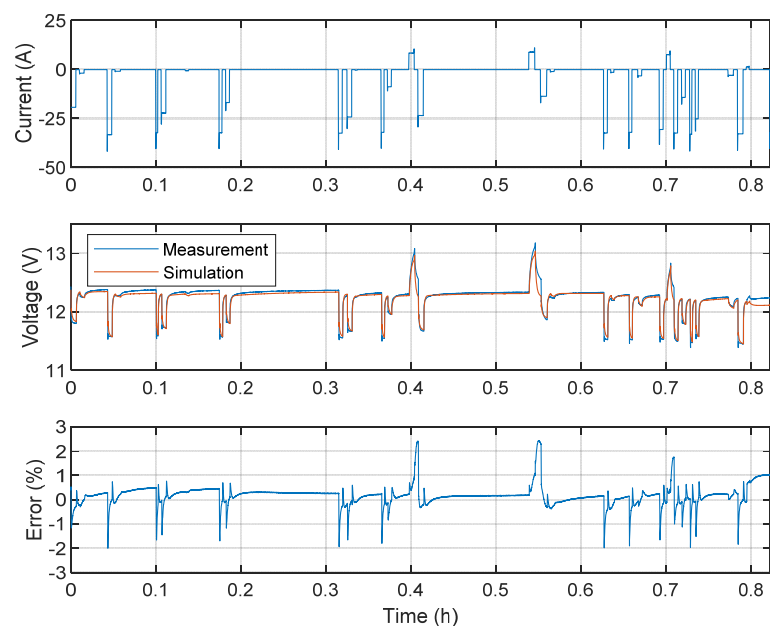


Figure 13. New lead-acid battery validation test (100% SOH).

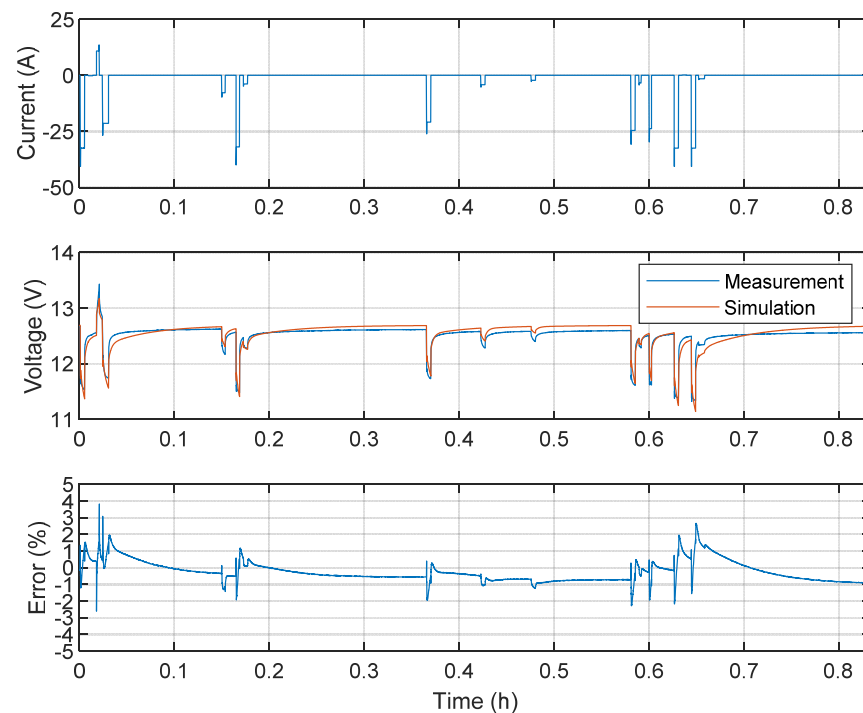


Figure 14. Aged lead-acid battery validation test (40% SOH).

Figure 13 shows that the maximum error for the new lead-acid battery was 2.5%, which was obtained in the charge pulses. In contrast, the maximum error obtained in the discharge pulses was 2%. In the case of the aged battery, (Figure 14), an error of 3.8% was observed in charge pulses, and 2.6% in the discharge pulses.

The relative error results for all tests (pulse characterization and validation) and battery technologies are presented in Table 2.

Table 2. Relative error results in pulse characterization and validation tests for lithium-ion and lead-acid batteries.

Technology	Test	Max. Error (Charge)	Max. Error (Discharge)
Lithium-ion	Pulse characterization	1.75%	1.8%
	Validation	0.75%	1.85%
Lead-acid 100% SOH	Pulse characterization	4%	2.5%
	Validation	2.5%	2%
Lead-acid 40% SOH	Pulse characterization	4%	2.7%
	Validation	3.8%	2.6%

7. Conclusions

A single behavioral model to predict the battery performance of different storage technologies for different applications was developed by implementing an ECM with two time constants. In addition, a parametrization test based on capacity and pulse tests, as well as model parameter extraction and estimation methods, has been presented.

The results show that the model can be used to represent the real behavior of different energy storage technologies and different aging states. In the present study, lithium-ion and lead-acid batteries were analyzed due to their current widespread use. Furthermore, in the case of lead-acid technology, the tests were performed for two different SOHs.

The variables considered in the validation and characterization tests were the current rate, the SOC and the SOH. The methodology presented considers the current rate and the SOC, and by testing batteries at different SOHs, the age of the battery can be considered.

In this way, it is possible to generate an adaptive model across the lifetime. In future studies, more characterization and validation tests will be carried out with batteries exposed to different temperature conditions in order to validate the developed methodology and models.

The results for the pulse characterization and validation tests of both technologies are set out in Table 2, which shows that the lithium-ion technology achieved better results in terms of relative error. The best results were obtained for an SOC range of 20 to 80%, the most interesting range for the analyzed traction application.

Author Contributions: Conceptualization, O.A. and E.A.; methodology, O.A.; software, O.A. and E.A.; validation, J.Y. and U.N.; formal analysis, O.A.; investigation, O.A.; resources, U.I.; data curation, E.A.; writing—original draft preparation, O.A. and E.A.; writing—review and editing, U.I., A.M., R.S. and I.G.; visualization, U.I. and A.M.; supervision, U.I.; project administration, U.I.; funding acquisition, U.I. All authors have read and agreed to the published version of the manuscript.

Funding: This research received no external funding.

Institutional Review Board Statement: Not applicable.

Informed Consent Statement: Not applicable.

Data Availability Statement: The data relevant with this study can be accessed by contacting the corresponding author.

Conflicts of Interest: The authors declare no conflict of interest.

References

1. Foray, D.; Goddard, J.; Beldarrain, X.G.; Landabaso, M.; McCann, P.; Morgan, K.; Nauwelaers, C.; Ortega-Argilés, R. *Guide to Research and Innovation Strategies for Smart Specialization (RIS3)*; European Commission: Brussels, Belgium, 2012; ISBN 978-92-79-25094-1.
2. Pillot, C. *Comparing Li-Ion to Lead-Acid Batteries & Other Storage Options: Future Predictions*; AVICENNE Energy: Cleveland, OH, USA, 2017.
3. Heydari, S.; Fajri, P.; Rasheduzzaman, M.; Sabzehgar, R. Maximizing Regenerative Braking Energy Recovery of Electric Vehicles Through Dynamic Low-Speed Cutoff Point Detection. *IEEE Trans. Transp. Electrification* **2019**, *5*, 262–270. [[CrossRef](#)]
4. Iannuzzi, D. Improvement of the energy recovery of traction electrical drives using supercapacitors. In Proceedings of the 2008 13th International Power Electronics and Motion Control Conference, Poznan, Poland, 1–3 September 2008; pp. 1469–1474. [[CrossRef](#)]
5. Pimm, A.J.; Cockerill, T.T.; Taylor, P.G. The potential for peak shaving on low voltage distribution networks using electricity storage. *J. Energy Storage* **2018**, *16*, 231–242. [[CrossRef](#)]
6. Saez-De-Ibarra, A.; Milo, A.; Gaztanaga, H.; Etxeberria-Otadui, I.; Rodriguez, P.; Bacha, S.; Debusschere, V. Analysis and comparison of battery energy storage technologies for grid applications. In Proceedings of the 2013 IEEE Grenoble Conference, Grenoble, France, 16–20 June 2013; pp. 1–6. [[CrossRef](#)]
7. Koniak, M.; Czerepicki, A. Selection of the battery pack parameters for an electric vehicle based on performance requirements. *IOP Conf. Ser. Mater. Sci. Eng.* **2017**, *211*. [[CrossRef](#)]
8. Xiong, R.; Cao, J.; Yu, Q.; He, H.; Sun, F. Critical Review on the Battery State of Charge Estimation Methods for Electric Vehicles. *IEEE Access* **2017**, *6*, 1832–1843. [[CrossRef](#)]
9. Dai, H.; Wei, X.; Sun, Z. A new SOH prediction concept for the power lithium-ion battery used on HEVs. In Proceedings of the 2009 IEEE Vehicle Power and Propulsion Conference, Dearborn, MI, USA, 7–10 September 2009; pp. 1649–1653. [[CrossRef](#)]
10. Dees, D.W.; Battaglia, V.S.; Bélanger, A. Electrochemical modeling of lithium polymer batteries. *J. Power Sources* **2002**, *110*, 310–320. [[CrossRef](#)]
11. Smith, K.A.; Rahn, C.D.; Wang, C.Y. Model-based electrochemical estimation and constraint management for pulse operation of lithium ion batteries. *IEEE Trans. Control Syst. Technol.* **2010**, *18*, 654–663. [[CrossRef](#)]
12. Chen, M.; Member, S.; Rinc, G.A. Accurate Electrical Battery Model Capable of Predicting Runtime and I–V Performance. *IEEE Trans. Energy Convers.* **2006**, *21*, 504–511. [[CrossRef](#)]
13. Bizeray, A.M.; Kim, J.; Duncan, S.R.; Howey, D.A. Identifiability and Parameter Estimation of the Single Particle Lithium-Ion Battery Model. *IEEE Trans. Control Syst. Technol.* **2019**, *27*, 1862–1877. [[CrossRef](#)]
14. Do, D.V.; Forgez, C.; El Kadri Benkara, K.; Friedrich, G. Impedance observer for a Li-ion battery using Kalman filter. *IEEE Trans. Veh. Technol.* **2009**, *58*, 3930–3937. [[CrossRef](#)]
15. Chiasserini, C.F.; Rao, R.R. Energy efficient battery management. *IEEE J. Sel. Areas Commun.* **2001**, *19*, 1235–1245. [[CrossRef](#)]
16. Zhang, L.; Peng, H.; Ning, Z.; Mu, Z.; Sun, C. Comparative research on RC equivalent circuit models for lithium-ion batteries of electric vehicles. *Appl. Sci.* **2017**, *7*, 1002. [[CrossRef](#)]

17. Ahmed, R.; Gazzarri, J.; Onori, S.; Habibi, S.; Jackey, R.; Rzemien, K.; Tjong, J.; Lesage, J. Model-Based Parameter Identification of Healthy and Aged Li-ion Batteries for Electric Vehicle Applications. *SAE Int. J. Altern. Powertrains* **2015**, *4*. [[CrossRef](#)]
18. Hu, X.; Li, S.; Peng, H. A comparative study of equivalent circuit models for Li-ion batteries. *J. Power Sources* **2012**, *198*, 359–367. [[CrossRef](#)]
19. Liu, K.; Li, K.; Peng, Q.; Zhang, C. A brief review on key technologies in the battery management system of electric vehicles. *Front. Mech. Eng.* **2019**, *14*, 47–64. [[CrossRef](#)]
20. Rahmoun, A. Mathematical Modeling and Analysis of a Battery Energy Storage System for Microgrids. Ph.D. Thesis, Tallinn University of Technology, Tallinn, Estonia, 2017.
21. Zhan, C.J.; Wu, X.G.; Kromlidis, S.; Ramachandaramurthy, V.K.; Barnes, M.; Jenkins, N.; Ruddell, A.J. Two electrical models of the lead-acid battery used in a dynamic voltage restorer. *IEE Proc. Commun.* **2003**, *150*, 175–182. [[CrossRef](#)]
22. Wu, X.; Li, X.; Du, J. State of Charge Estimation of Lithium-Ion Batteries over Wide Temperature Range Using Unscented Kalman Filter. *IEEE Access* **2018**, *6*, 41993–42003. [[CrossRef](#)]
23. Marchildon, J.; Doumbia, M.L.; Agbossou, K. SOC and SOH characterisation of lead acid batteries. In Proceedings of the IECON 2015—41st Annual Conference of the IEEE Industrial Electronics Society, Yokohama, Japan, 9–12 November 2015; pp. 1442–1446. [[CrossRef](#)]
24. Shamsi, M.H. Analysis of an Electric Equivalent Circuit Model of a Li-Ion Battery to Develop Algorithms for Battery States estimation. Masterprogrammet i Energiteknik Master Programme in Energy Technology. 2016. Available online: <https://www.diva-portal.org/smash/record.jsf?pid=diva2%3A946064&dswid=1360> (accessed on 1 November 2021).
25. Wang, W.; Chung, H.S.; Zhang, J. Near-real-time parameter estimation of an electrical battery model with multiple time constants and SOC-dependent capacitance. *IEEE Trans. Power Electron.* **2014**, *29*, 5905–5920. [[CrossRef](#)]
26. Lynch, W.A.; Salameh, Z.M. Electrical component model for a nickel-cadmium electric vehicle traction battery. In Proceedings of the 2006 IEEE Power Engineering Society General Meeting, Montreal, QC, Canada, 18–22 June 2006; p. 5.
27. Rahmoun, A.; Biechl, H. Modelling of Li-ion batteries using equivalent circuit diagrams. *Prz. Elektrotechniczny* **2012**, *88*, 152–156.
28. Garayalde Perez, E. Hybrid Energy Storage Systems via Power Electronic Converters. 2019. Available online: <http://ebiltegia.mondragon.edu/xmlui/handle/20.500.11984/1783> (accessed on 1 November 2021).
29. Ouyang, Q.; Wang, Z.; Liu, K.; Xu, G.; Li, Y. Optimal Charging Control for Lithium-Ion Battery Packs: A Distributed Average Tracking Approach. *IEEE Trans. Ind. Inform.* **2020**, *16*, 3430–3438. [[CrossRef](#)]
30. Liu, K.; Zou, C.; Li, K.; Wik, T. Charging Pattern Optimization for Lithium-Ion Batteries With an Electrothermal-Aging Model. *IEEE Trans. Ind. Inform.* **2018**, *14*, 5463–5474. [[CrossRef](#)]
31. Thunder Sky Winston Battery “Lithium ion”, LFP040AHA Cell Datasheet. Available online: <https://en.winston-battery.com/> (accessed on 1 June 2021).
32. Glaize, C.; Geniès, S. *Lithium Batteries and Other Electrochemical Storage Systems*; John Wiley & Sons: Hoboken, NJ, USA, 2013; ISBN 9781848214965.
33. Yuasa “VRLA Battery”, NPC24-12 Datasheet. Available online: <https://www.yuasa.es/batteries/industriales/golf-mobility/npc24-12i-npc24-12i.html> (accessed on 1 June 2021).